

Supplementary Information

Enhanced Catalytic Activity Induced by Defects in Mesoporous Ceria Nanotubes

Guomin Hua¹, Lide Zhang^{1*}, Guangtao Fei¹, Ming Fang¹

¹ Key Laboratory of Materials Physics and Anhui Key Laboratory of Nanomaterials and Nanostructures, Institute of Solid State Physics, Chinese Academy of Sciences, Hefei, 230031 Anhui, People's Republic of China

Phone: +86-551-5591420, Fax: +86-551-5592753

Email: ldzhang@issp.ac.cn

Content

- 1. Information on the characterization of mesoporous polycrystalline ceria nanotubes**
- 2. Surface area measurement of mesoporous polycrystalline ceria nanotubes**
- 3. Raman scattering spectrum of mesoporous polycrystalline ceria nanotubes**
- 4. Reference**

1. Information on the characterization of mesoporous polycrystalline ceria nanotubes

The schematic illustration of synthetic procedures for the mesoporous ceria nanotubes are presented in figure S1 a. In the first step, the ZnO nanorods as templates are prepared by hydrothermal synthesis. In the second step, amorphous Ceria nanoshell is covered on the surface of obtained ZnO nanorod templates by the ultrasonic assisted successive ionic layer adsorption and reaction (UASILAR) method which is followed by an annealing treatment to force the amorphous Ceria nanoshell to crystallize on the ZnO nanorods. In the third step, the chemical etching is adopted to remove the ZnO nanorod templates to form the mesoporous ceria nanotubes. The phases of the products obtained are shown in figure S1 b. At the first step, the ZnO nanorods are of wurtzite structure. At the second step, the phase of the products contains only wurtzite ZnO and fluoride ceria, no other phases are observed. At the third step, the obtained products are simply fluoride ceria. The morphologies of ZnO nanorod obtained at the first step and the mesoporous ceria nanotubes obtained at the third step are shown in figures S1 c and S1 d, respectively. The mesoporous ceria nanotubes can effectively inherit the size features of ZnO nanorods.

From the TEM images shown in figure S2, the structural features of the products obtained at different stages can be observed. As shown in figure S2 a, the as-prepared ZnO nanorods have smooth surfaces and uniform size distribution. After the mesoporous Ceria nanoshell covered on the ZnO nanorods by the UASILAR methods and annealing treatment (Figure S2 b), the surfaces of nanorods become rough. The transversal element distribution shown in figure S2 c reveals core/shell structural features where the inner core is ZnO and the outer shell is ceria. The High-Resolution TEM (HRTEM) image presented in figure S2 d shows the ZnO nanorod is tightly wrapped by ceria nanoshell. As

shown in figure S2 e, the mesoporous ceria nanotubes can be obtained after the removal of ZnO nanorods, the HRTEM image of mesoporous ceria nanotubes shown in figure S2 f reveals that the nanotube walls is consisted of small grain size, high density of grain boundaries and mesopores, and the internal surface of the nanotube is smoother than the external surface. It may be result from the crystallization process of ceria nanoshells on ZnO nanorods. The Selected Area Electron Diffraction (SAED) pattern indicates the as-prepared mesoporous ceria nanotubes are polycrystalline.

To meet the requirements of the state-of-the-art nanotechnology like fuel cells, solar cells, chemical and biological sensors, the mesoporous polycrystalline ceria nanotubes can be assembled into order arrays on the substrate. The as-prepared nanoarrays were presented in figure S3.

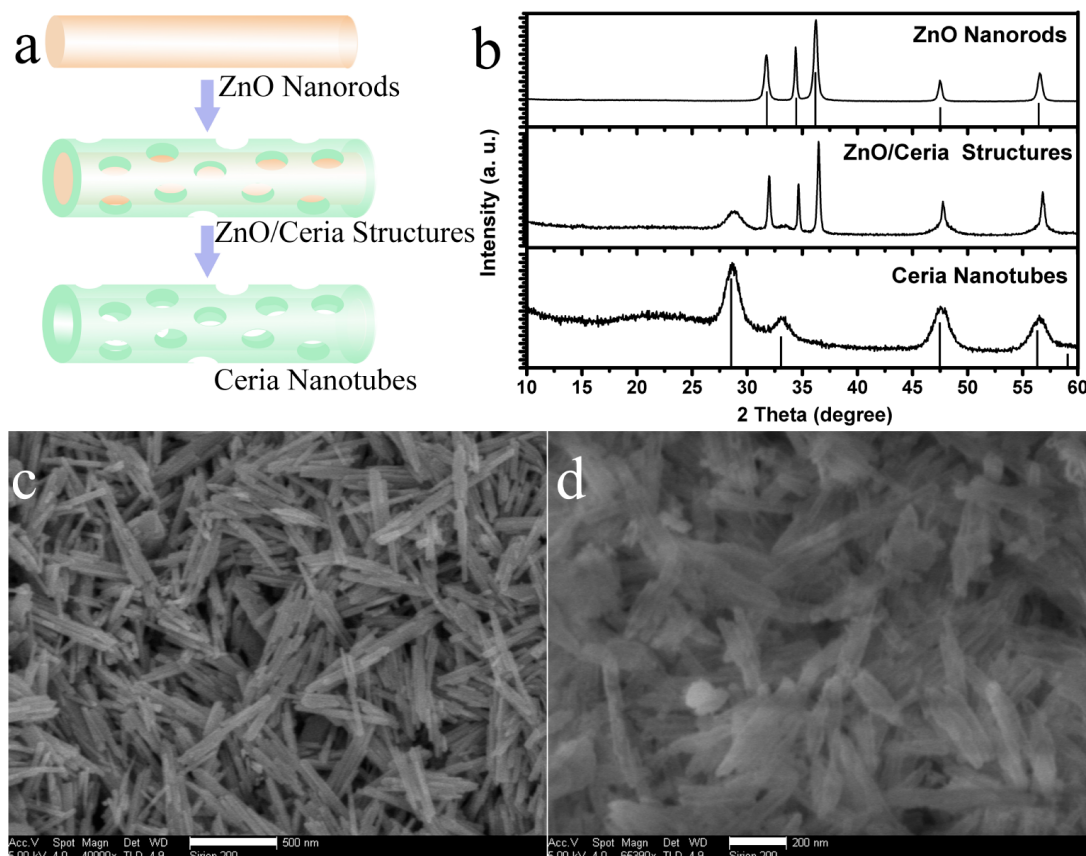


Figure S1. (a) The schematic illustration of the mesoporous ceria nanotube preparation via ZnO nanorod template synthesis together with ultrasonic assisted SILAR covering method; (b) The XRD spectra of ZnO nanorods prepared by hydrothermal synthesis, ceria nanoshell covered on the surface of ZnO nanorods after the thermal treatment at 500 °C and the mesoporous ceria nanotubes after the removal of ZnO nanorods, respectively; (c) FESEM images of ZnO nanorods, scale bar: 500nm; (d) FESEM images of mesoporous ceria nanotubes, scale bar: 200nm.

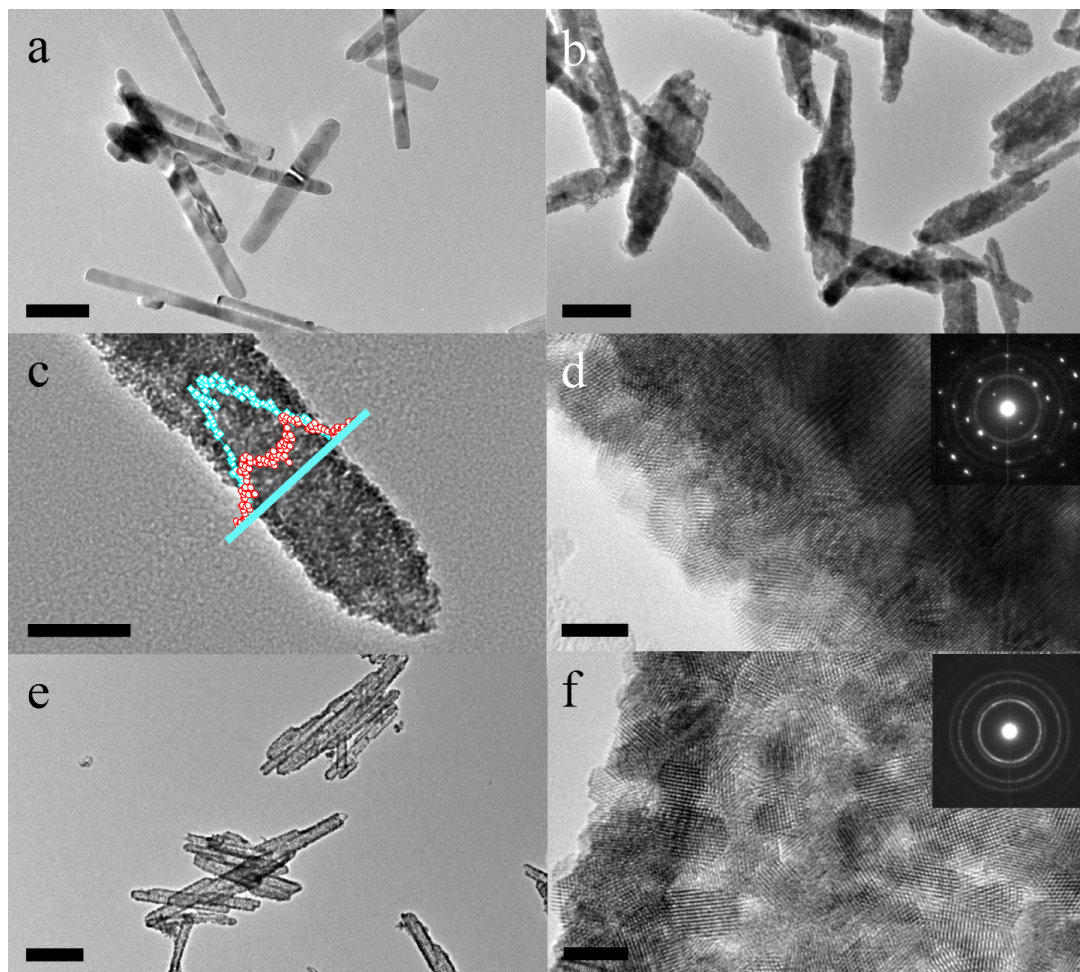


Figure S2. (a) The TEM image of the ZnO nanorods prepared by hydrothermal synthesis, scale bar: 100nm; (b) The TEM image of ceria nanoshell covered on the surface of ZnO nanorods prepared by ultrasonic assisted SILAR method, scale bar: 200nm; (c) The transversal element distribution of ceria nanoshell covered on the surface of ZnO nanorods, red○: cerium element, green□: zinc element, scale bar: 50nm; (d) The HR-TEM image of ceria nanoshell covered on the surface of ZnO nanorods, inset: SAED pattern, scale bar: 5nm; (e) The TEM image of mesoporous ceria nanotubes after the removal of ZnO nanorods, scale bar: 200nm; (f) The HR-TEM image of mesoporous ceria nanotubes, inset: SAED pattern, scale bar: 5nm.

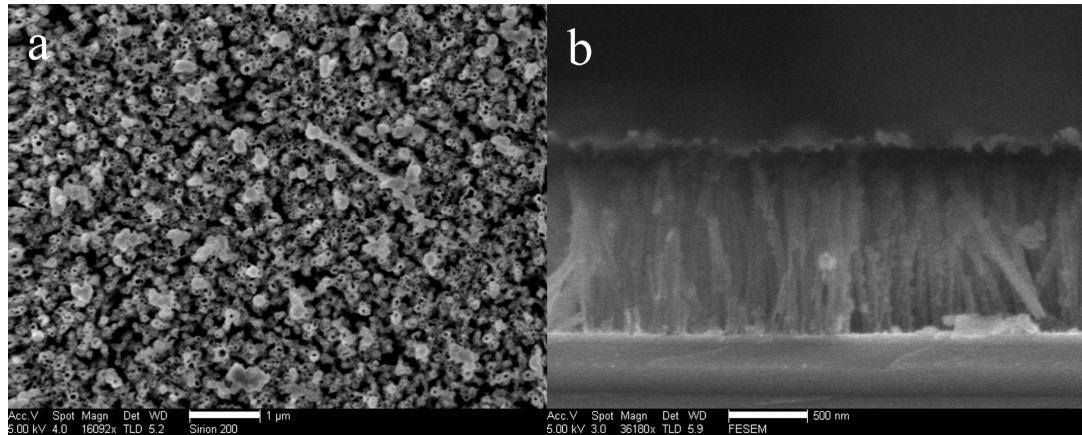


Figure S3. The morphologies of the ordered nanoarrays of mesoporous polycrystalline ceria nanotubes.
(a) Top view image, scale bar: 1μm; (b) cross-section view image, scale bar: 500nm.

2. Surface area measurement of mesoporous polycrystalline ceria nanotubes

The structural feature of mesoporous ceria nanotubes after calcinations at 500 °C was characterized by the nitrogen adsorption. From the relative pressure (P/P_0) rang of 0.05~0.3 in the nitrogen adsorption-desorption isotherms (figure S4), the surface area of the mesoporous ceria nanotubes is calculated about $109\text{ m}^2/\text{g}$, and the surface area of the commercial ceria powder is about $42\text{ m}^2/\text{g}$ according to the Brunauer-Emmett-Teller method. The H_2 -type hysteresis loop in the adsorption-desorption isotherm suggests the mesoporous feature of the as-prepared ceria nanostructures. And the size distribution reveals that two types of mesopores contribute to the large surface area, one is the mesopores of about 2.1 nm in size which is formed on the ceria nanotube walls, and another is the mesopores of about 23 nm in size which is correspond to the hollow tubes of ceria nanotubes after the removal of ZnO nanorod. The surface area of mesoporous ceria nanotube is effectively enlarged.

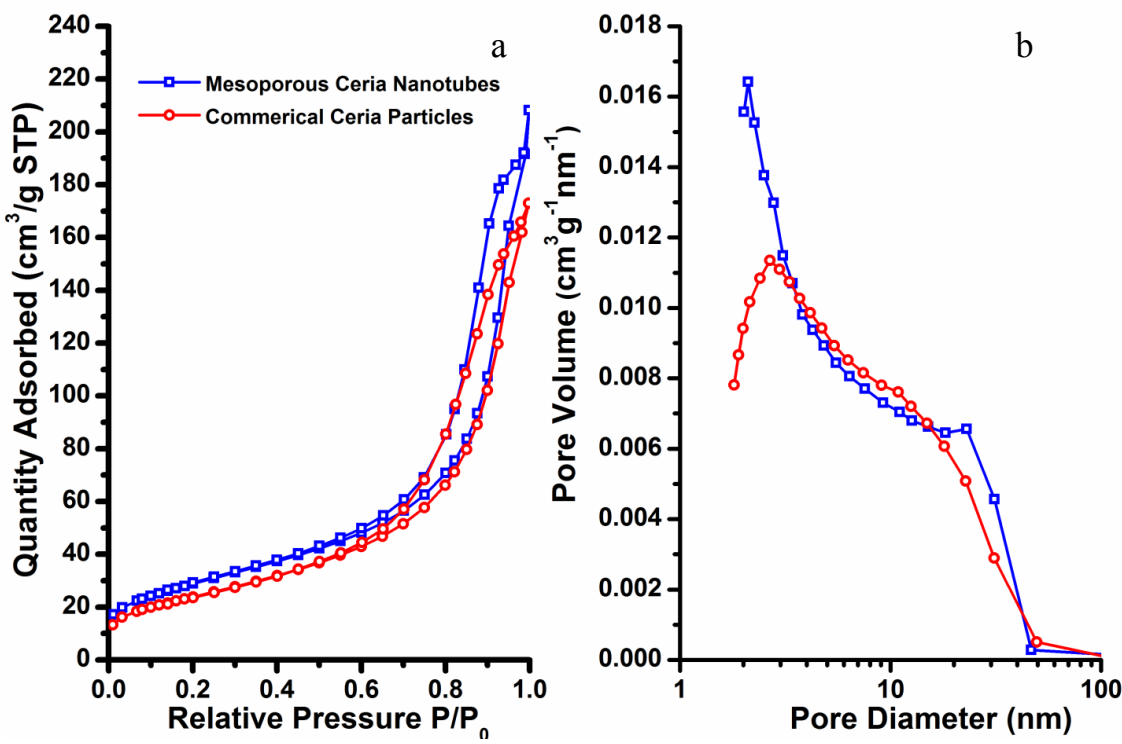


Figure S4. The structural feature of ceria nanotubes after calcinations at 500 °C. (a) Nitrogen adsorption-desorption isotherms and (b) mesopore size distribution calculated by the adsorption branch of the isotherms.

3. Raman scattering spectrum of mesoporous polycrystalline ceria nanotubes

Raman scattering spectra of the mesoporous polycrystalline ceria nanotubes and stoichiometric ceria particles are collected in the backscattering configuration from 300 to 1200 cm^{-1} and presented in figure S5. Besides the first-order Raman band near 464 cm^{-1} and second-order bands were observed at 598 cm^{-1} and 1174 cm^{-1} , oxygen species related Raman band at 966 cm^{-1} and 1123 cm^{-1} can be

observed in mesoporous polycrystalline ceria nanotubes, which is corresponded to formation of peroxides (O_2^{2-}) and superoxide (O_2^-) respectively by oxygen adsorption on surfaces¹. The formation of active oxygen species can be attributed to the high density of one electron defects of Ce³⁺ ions distributed on the surface of mesoporous polycrystalline ceria nanotubes^{2,3}.

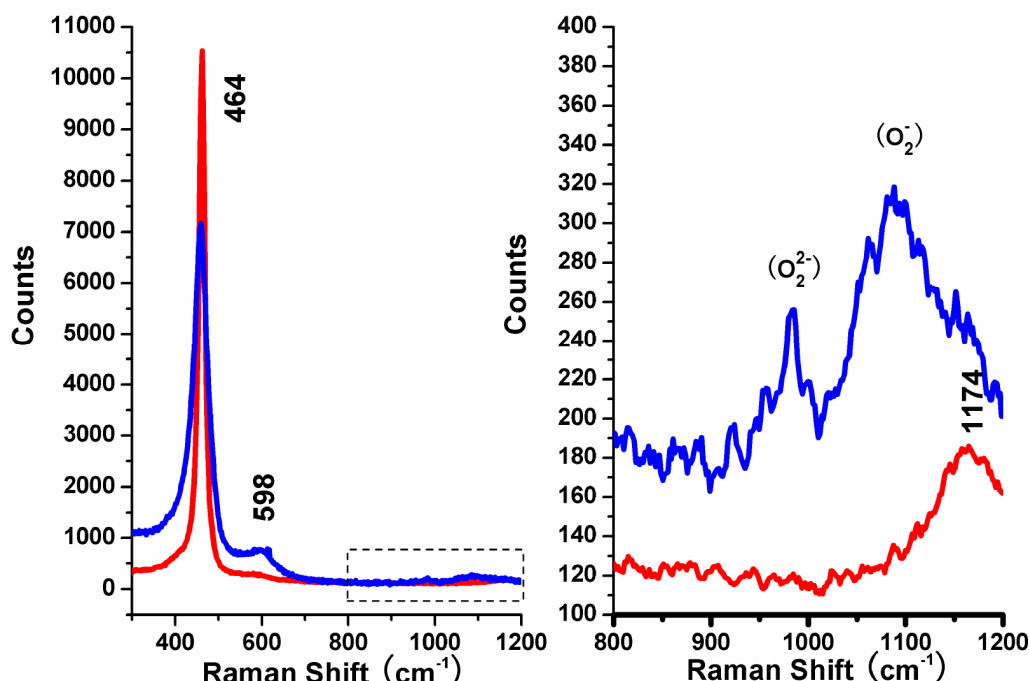


Figure S5. (a) Raman spectra of the mesoporous polycrystalline ceria nanotubes (blue curve) and stoichiometric ceria particles (red curve); (b) the magnified Raman spectra corresponding to the range of 800 to 1200cm⁻¹ as the rectangular dash line pointed out in (a).

4. Reference

- ¹ Guzman, J., Carrettin, S., and Corma, A., Spectroscopic evidence for the supply of reactive oxygen during CO oxidation catalyzed by gold supported on nanocrystalline CeO₂. *Journal of the American Chemical Society* **127** (10), 3286 (2005).
- ² Yao, H. C. and Yao, Y. F. Y., Ceria in Automotive Exhaust Catalysts .1. Oxygen Storage. *Journal of Catalysis* **86** (2), 254 (1984).
- ³ Guzman, J. et al., CO oxidation catalyzed by supported gold: Cooperation between gold and nanocrystalline rare-earth supports forms reactive surface superoxide and peroxide species. *Angewandte Chemie-International Edition* **44** (30), 4778 (2005).